



The telomerase inhibitor PinX1 is a major haploinsufficient tumor suppressor essential for chromosome stability in mice

Xiao Zhen Zhou,¹ Pengyu Huang,¹ Rong Shi,¹ Tae Ho Lee,¹ Gina Lu,¹ Zhihong Zhang,¹ Roderick Bronson,² and Kun Ping Lu¹

¹Department of Medicine, Beth Israel Deaconess Medical Center, and ²Rodent Histopathology Core, Harvard Medical School, Boston, Massachusetts, USA.

Telomerase is activated in most human cancers and is critical for cancer cell growth. However, little is known about the significance of telomerase activation in chromosome instability and cancer initiation. The gene encoding the potent endogenous telomerase inhibitor PinX1 (PIN2/TRF1-interacting, telomerase inhibitor 1) is located at human chromosome 8p23, a region frequently exhibiting heterozygosity in many common human cancers, but the function or functions of PinX1 in development and tumorigenesis are unknown. Here we have shown that PinX1 is a haploinsufficient tumor suppressor essential for chromosome stability in mice. We found that PinX1 expression was reduced in most human breast cancer tissues and cell lines. Furthermore, *PinX1* heterozygosity and *PinX1* knockdown in mouse embryonic fibroblasts activated telomerase and led to concomitant telomerase-dependent chromosomal instability. Moreover, while *PinX1*-null mice were embryonic lethal, most *PinX1*^{+/-} mice spontaneously developed malignant tumors with evidence of chromosome instability. Notably, most *PinX1* mutant tumors were carcinomas and shared tissues of origin with human cancer types linked to 8p23. *PinX1* knockout also shifted the tumor spectrum of p53 mutant mice from lymphoma toward epithelial carcinomas. Thus, *PinX1* is a major haploinsufficient tumor suppressor essential for maintaining telomerase activity and chromosome stability. These findings uncover what we believe to be a novel role for *PinX1* and telomerase in chromosome instability and cancer initiation and suggest that telomerase inhibition may be potentially used to treat cancers that overexpress telomerase.

Introduction

It has become evident that inactivation of tumor suppressor genes due to gene alterations, notably loss of heterozygosity (LOH), plays a major role in the development of common human adult cancers, with breast cancer as a notable example (1–3). Chromosome 8p23 is one of the most frequent LOH regions in common human adult epithelial malignancies, including breast, liver, lung, and gastrointestinal cancers. For example, up to 70% of hepatocellular carcinomas (4–8) and 60% of human gastric cancer (9) exhibit LOH at 8p23 near the marker D8S277. 8p23 is also a common integration site for HBV, a well-known major risk factor in liver cancer (5, 10). Similarly, LOH on 8p is found in up to 50% of breast carcinomas and is often associated with advanced tumor stage and aggressive histology (11–14). Although several tumor suppressors have been mapped to this region, including transcriptional factors Nkx3.1 at 8p21 and FEZ1/LZTS1 at 8p22 (15–17), even the combined rates of loss of these genes could not account for the extensive alterations seen in human tumors (16), indicating that major tumor suppressor gene or genes remain to be identified.

Telomerase is activated in most human cancers (18, 19). Telomerase elongates telomeres, which cap the ends of linear chromosomes and are essential for maintaining chromosome stability (20–25). Its activity is absent or very low in most normal human somatic cells so that telomeres shorten during each cell

division. However, telomerase activation is critical for transforming primary human cells (26) and for enabling transformed cells to escape from crisis (27, 28). Moreover, transgenic telomerase reverse transcriptase catalytic subunit (TERT) overexpression in mice induces tumors in a telomerase RNA component-dependent (TERC-dependent) manner (29–32) and also cooperates with p53 knockout in inducing spontaneous cancer development (31), analogically to telomerase knockout (33) or telomere deprotection (34). In addition, telomerase regulates DNA damage response (35, 36) and can also promote epithelial proliferation through transcriptional activation by serving as a cofactor (37). Telomerase activation is thus important for cancer cell growth. However, there is no genetic evidence linking telomerase activation to chromosome instability, making it difficult to link telomerase activation to cancer initiation. Moreover, while transcription of the telomerase catalytic subunit TERT is well known to be activated by deregulation of many oncogenes and tumor suppressors (38–41), little is known about the inhibition of telomerase activity and its significance in oncogenesis.

In mammalian cells, the ability of telomerase to elongate telomeres is regulated by telomere-associated proteins (24), including telomeric repeat binding factor 1 (TRF1) (42) and its associated proteins (43, 44), including PIN2/TRF1-interacting, telomerase inhibitor 1 (*PinX1*) (45). However, unlike other TRF1-binding proteins, *PinX1* is unique in that it can also directly bind to TERT and inhibit telomerase activity (45). Furthermore, inhibition of *PinX1* in human cancer cells increases telomerase activity, whereas *PinX1* overexpression has the opposite effect (45). Moreover, *PinX1* is recruited to telomeres by TRF1 and provides a critical link between TRF1 and telomerase inhibition to help maintain

Authorship note: Pengyu Huang, Rong Shi, and Tae Ho Lee contributed equally to this work.

Conflict of interest: The authors have declared that no conflict of interest exists.

Citation for this article: *J Clin Invest.* 2011;121(4):1266–1282. doi:10.1172/JCI43452.



telomeres at the optimal length (46). The ability of PinX1 to regulate telomerase and telomere length is conserved in yeast, rats, and fish (47–49). However, it is not known why such a telomerase inhibitor is needed *in vivo*.

Notably, the *PinX1* gene localizes to human chromosome 8p23 near the marker D8S277 (8, 45). Furthermore, PinX1 expression is reduced in approximately 40% of HBV-related liver cancer (8, 50). Moreover, PinX1 inhibition increases, whereas PinX1 overexpression suppresses, tumorigenicity of cancer cells (45). These results suggest that PinX1 might be a putative tumor suppressor. Subsequent PinX1 studies on human cancer samples provide some supportive evidence (9, 50) and contradictory results (51, 52). Furthermore, the interpretation of these expression results is complicated because they all used RT-PCR analyses that could detect other alternatively spliced PinX1 variants and a potential PinX1 pseudogene in the genome. Therefore, expression of PinX1 in human cancer tissues remains unclear. Moreover, there is no genetic evidence for any involvement of PinX1 in tumorigenesis.

To determine the role of PinX1 in cancer, we first examined PinX1 expression in human breast cancer tissues and cells and then generated PinX1 knockout or knockdown and telomerase knockout or knockdown to examine the impact of PinX1 on tumorigenesis *in vitro* and *in vivo*. Our results provide what we believe is the first evidence for PinX1 as a major haploinsufficient tumor suppressor essential for maintaining chromosome stability and link for the first time, to our knowledge, aberrant telomerase activation to chromosome instability and cancer initiation. These findings also suggest that telomerase inhibitors may be effective in treating cancers that overexpress telomerase.

Results

PinX1 expression is reduced in most human breast cancer tissues and cells. To examine the role of PinX1 in oncogenesis, we first used multiple methods to examine PinX1 expression in commonly used human breast cancer cell lines. PinX1 expression was readily detected in normal breast epithelial cell line MCF-10A, but its expression was reduced to variable degrees in 6 out of 7 breast cancer cell lines examined, as determined by quantitative RT-PCR (qRT-PCR) analysis of a *PinX1* mRNA fragment covering all the 7 coding exons (Figure 1A) and confirmed by immunoblotting (Figure 1B) and immunostaining (Figure 1C) analyses using affinity-purified anti-C-terminal PinX1 antibodies that we generated. Immunostaining also confirmed that PinX1 was localized to nucleoli in addition to telomeres (Figure 1C), as shown (45, 47). These results indicate that PinX1 expression is reduced in most human breast cancer cell lines.

Next, to examine PinX1 expression in human breast cancer tissues, we subjected serial sections of tissue microarrays of 10 normal and 49 tumor specimens to immunohistochemistry to determine PinX1 expression in a semiquantitative manner (Figure 1D). Out of 10 normal breast tissues, 9 contained high levels and 1 expressed medium levels of PinX1 (Figure 1D and Table 1). However, in breast cancer tissues, only 10% of specimens expressed high levels of PinX1, whereas 41% and 49% of samples contained medium and low levels of PinX1, respectively (Figure 1D and Table 1). The differences in PinX1 expression between normal and breast cancer tissues were highly significant, as determined by the Spearman's rank correlation test ($P < 0.01$). Thus, PinX1 expression was reduced in most breast cancer tissues and cells examined.

While PinX1-null mice are embryonic lethal, PinX1 heterozygous knockout reduces PinX1 levels and increases telomerase activity and telomere length in mouse embryonic fibroblasts and mice. To determine the significance of PinX1 downregulation in oncogenesis, we generated PinX1-knockout mice. To create the PinX1 targeting construct, we subcloned 3 genomic fragments of PINX1 into the pKOII vector (Figure 2A), which was linearized and electroporated into ES cells, resulting in 2 independent ES clones that had the correct recombination (rec) of the PinX1 targeting vector at the PinX1 locus (Figure 2A), as confirmed both by PCR and Southern analyses (data not shown). Both *PinX1*^{+rec} ES clones were injected into mouse blastocysts, giving rise to 9 and 2 chimeric mice, which were designated as A and B lines, respectively, and contained the germline transmitted PinX1^{rec} allele in both lines upon backcrossing. To generate PinX1-knockout mice, we crossed heterozygous *PinX1*^{+rec} mice with CMV-Cre transgenic mice to generate a conventional PinX1-knockout allele (PinX1) (Figure 2A), as determined by Southern blot (Figure 2B) and PCR analyses (Figure 2C), as described (53). Of note, all the phenotypes as described here are found both in A and B lines of mice, indicating that it is unlikely that the phenotypes are due to a random integration of the construct.

We failed to obtain any *PinX1*^{-/-} mice from intercrosses with *PinX1*^{+/-} mice (Supplemental Figure 1E; supplemental material available online with this article; doi:10.1172/JCI43452DS1). Although no obvious differences were observed among E8.5 embryos with different PinX1 genotypes (Supplemental Figure 1A), *PinX1*^{-/-} embryos were much smaller and very pale at E9.5 and E10.5, appearing devoid of a blood supply and often without a detectable heartbeat (Supplemental Figure 1, B and C). There were no live *PinX1*^{-/-} embryos at E11.5 or E12.5, whereas *PinX1*^{+/-} embryos appeared normal (Supplemental Figure 1, D and E). *PinX1*^{+/-} mice were viable and appeared to thrive, but their ratio to *PinX1*^{+/+} mice was close to 1:1 (Supplemental Figure 1E). Because no neonatal lethality was detected, a fraction of the *PinX1*^{+/-} embryos had likely died *in utero*. Thus, PinX1 is essential for embryonic development, as are other telomere-related proteins, including TRF1 (54) and Tin2 (55).

PinX1^{+/-} mice were viable and appeared to thrive, but their ratio compared with *PinX1*^{+/+} mice was only 48%:52% (Supplemental Figure 1E). Because no neonatal lethality was detected, a fraction of the *PinX1*^{+/-} embryos must have died *in utero*, suggesting a haploinsufficiency. To further examine this possibility, we used qRT-PCR and immunoblotting to determine levels of *PinX1* mRNA and protein in mouse adult tissues, embryos at E9.5, and mouse embryonic fibroblasts (MEFs) derived from *PinX1*^{+/+}, *PinX1*^{+/-}, and *PinX1*^{fl/fl} embryos at E12.5. Compared with WT controls, *PinX1* mRNA was reduced by approximately 60% in *PinX1*^{+/-} embryos, but was not detected in *PinX1*^{-/-} embryos (Figure 2D). PinX1 protein in *PinX1*^{+/-} livers and MEFs was reduced by 60%–70% (Figure 2, E and F). These results indicate gene-dose-dependent PinX1 expression *in vitro* and *in vivo*.

To examine whether reducing PinX1 affects telomerase activity, we compared telomerase activity in *PinX1*^{+/+} and *PinX1*^{+/-} MEFs and testis tissues using the standard telomere repeat amplification protocol (TRAP) assay. Telomerase activity in multiple independent *PinX1*^{+/-} MEF lines (Figure 2, G and H, and Supplemental Figure 2, A and B) and testis tissues from 3 mice (Figure 2, I and J) was reproducibly increased by roughly 2-fold, compared with *PinX1*^{+/+} controls. Furthermore, similar increases in

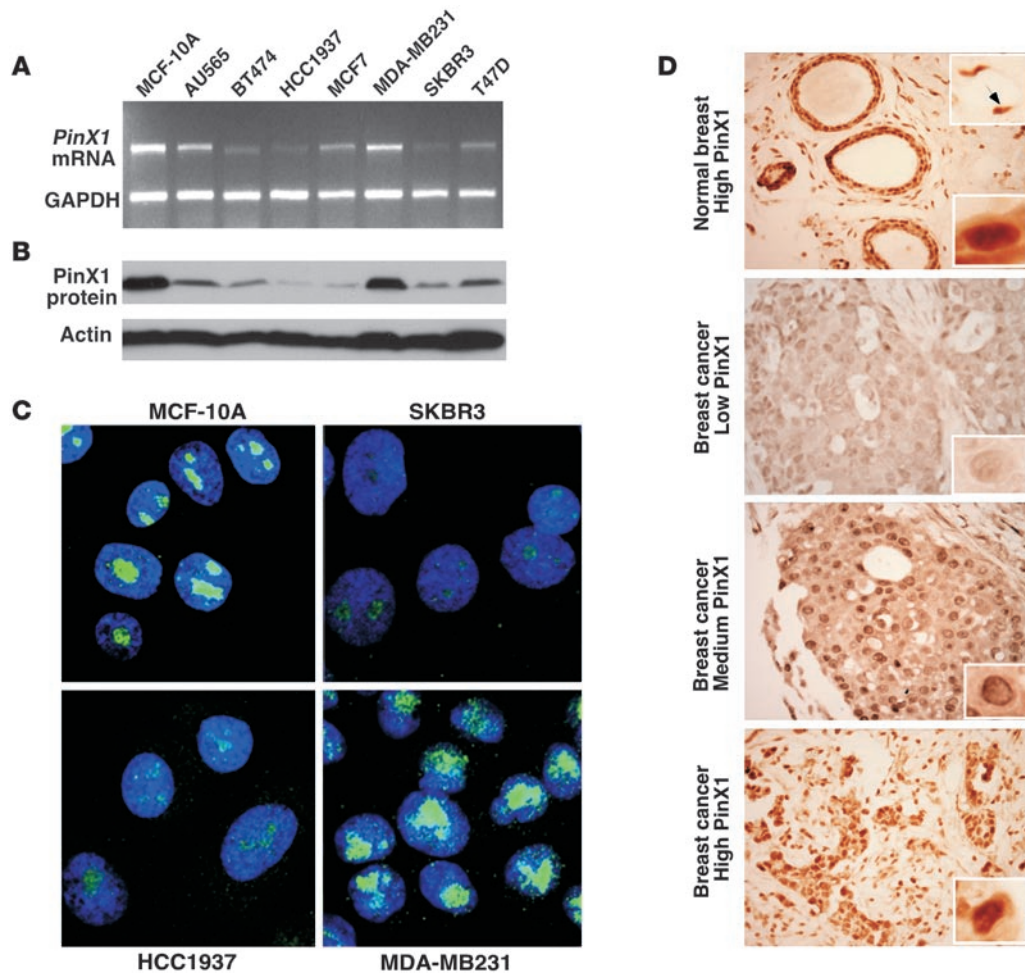


Figure 1

PinX1 expression is reduced in most human breast cancer tissues and cell lines. (A–C) PinX1 reduction in human breast cancer cell lines. Human normal and cancerous breast cell lines were subjected to qRT-PCR amplification of a 1.0-kb *PinX1* mRNA fragment covering all the 7 coding exons, with GAPDH as a control (A), to immunoblotting with anti-PinX1 antibodies with actin as a control (B), and immunofluorescence staining with anti-PinX1 antibodies (C). Original magnification, $\times 63$. (D) PinX1 reduction in human breast cancer tissues. Serial sections of tissue microarrays of 10 normal and 49 tumor breast specimens were subjected to immunohistochemistry using anti-PinX1 antibodies. In each sample, PinX1 expression was semiquantified in a double-blind manner as high, medium, or low according to the standards presented in D and summarized in Table 1. Original magnification, $\times 20$; $\times 40$ (insets).

telomerase activity were observed when various amounts of proteins were added to the assays (Figure 2, G and H). This small telomerase increase might be expected given that these normal cells and tissues do not express much telomerase, since PinX1 depletion by 70% leads to an approximately 5-fold increase in telomerase activity in HT1080 cancer cells (45). Thus, PinX1 heterozygous knockout results in a reproducible increase in telomerase activity in vitro and in vivo.

To further determine whether this small telomerase activation is functionally relevant, we examined whether it affects telomere length in PinX1 heterozygous knockout MEFs and mice over time. Primary *PinX1*^{+/+} and *PinX1*^{+/-} MEFs were continuously cultured for approximately 30 passages (~90 population doublings [PD]) using the classic 3T3 protocol (56), and then their telomere lengths were assayed at early and late passages (3–5 and 30 passages, respectively) using quantitative FISH (qFISH) and telomere Southern blot. qFISH results showed that *PinX1*^{+/+} and

PinX1^{+/-} MEFs had similar telomeric signal intensity at early passage (Figure 3, A–C), but *PinX1*^{+/-} cells had stronger telomeric signal intensity at late passage, with the average telomere fluorescence unit (TFU) being increased by approximately 40% (Figure 3, D–F). Although it is notoriously difficult to use telomere Southern blot to precisely measure such long mouse telomeres,

Table 1

PinX1 expression is reduced in most human breast cancer tissues

	PinX1 levels			Total
	Low	Medium	High	
Normal	0 (0%)	1 (10%)	9 (90%)	10 (100%)
Cancer	24 (49%)	20 (41%)	5 (10%)	49 (100%)

P < 0.01.

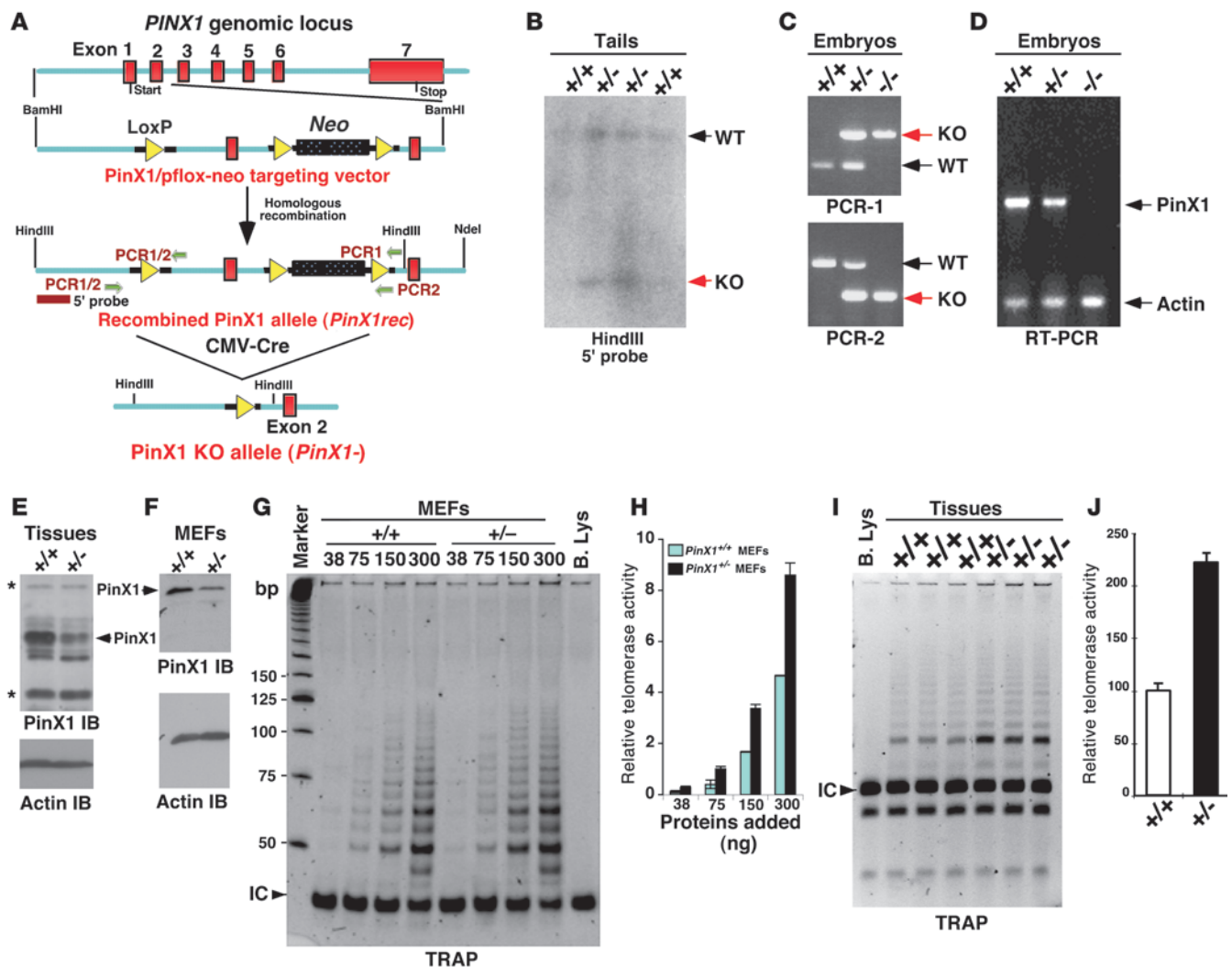


Figure 2

PinX1 expression is gene-dosage-dependent, and PinX1 heterozygous knockout reduces PinX1 expression and increases telomerase activity in vitro and in vivo. (A) Construction of the PinX1 targeting vector and deletion of the *PinX1* gene by Cre- and loxP-mediated homologous recombination. Cre-mediated deletion of the *PinX1*rec allele generates the *PinX1*⁻ allele. (B) Identification of PinX1-KO mice, as confirmed by genomic Southern analysis using a 5' probe. Black and red arrows point to the expected products of WT and KO alleles. (C) Identification of PinX1 KO mice by 2 different sets of PCR amplification using 3 primers each. (D) Gene-dosage-dependent expression of *PinX1* mRNA in mouse embryos, as determined by qRT-PCR amplification of 1-kb full-length *PinX1* mRNA in *PinX1*^{+/+}, *PinX1*^{+/-}, and *PinX1*^{-/-} embryos at E9.5. (E and F) Gene-dosage-dependent expression of PinX1 protein in liver tissues of adult *PinX1*^{+/+} and *PinX1*^{+/-} mice (E) and MEFs derived from *PinX1*^{+/+} and *PinX1*^{+/-} embryos at E12.5 (F), as determined by immunoblotting using anti-PinX1 antibodies. Unrelated proteins (E, marked with asterisks) and/or actin (E and F) were used as loading controls. (G and H) Elevated telomerase activity in primary *PinX1*^{+/-} MEFs. Telomerase-containing fractions were subject to the standard TRAP assay, stained with SYBR green (G), and semiquantified as ratios between telomerase products and the internal control (IC, arrow) (H). B. lys, boiled lysates. (I and J) Elevated telomerase activity in young *PinX1*^{+/-} testes tissues. Telomerase-containing fractions isolated from 3 *PinX1*^{+/-} or *PinX1*^{+/+} littermates were subject to the standard TRAP assay (I) and semiquantified, with *PinX1*^{+/+} telomerase activity being set at 100% (J). Data are represented as mean ± SD.

especially telomere lengthening, basically similar trends in telomere elongation were also observed in telomere Southern blot. *PinX1*^{+/-} and *PinX1*^{+/+} MEFs had again similar telomere lengths at early passage, but *PinX1*^{+/-} cells contained elongated telomeres at late passage in multiple independent clones, as evidenced by an increase in the telomeric hybridization signal and in the average TRF length by approximately 45% (Figure 3, G and H; *P* < 0.01). Thus, PinX1 knockout in MEFs leads to telomere elongation, further supporting telomerase activation.

To determine whether PinX1 knockout affects telomere-mediated DNA damage, *PinX1*^{+/+} and *PinX1*^{+/-} cells at early and late passages before and after γ -radiation were subjected to double staining with anti-p53BP1 and qFISH with a telomeric PNA probe, as described (57). Before irradiation, there were not any obvious p53BP1 foci in *PinX1*^{+/+} and *PinX1*^{+/-} cells at either early or late passage (Supplemental Figure 4A). In contrast, radiation induced prominent p53BP1 foci in these cells (Supplemental Figure 4B). However, the number or intensity of p53BP1 foci was



Figure 3

PinX1 heterozygous knockout leads to telomere elongation in MEFs and mice. (A–F) Telomere elongation in *PinX1*^{+/-} MEFs at late passage, as determined by qFISH. *PinX1*^{+/+} and *PinX1*^{+/-} MEFs at early (from 3 to 5) (A–C) and late (~30) (D–F) passage were fixed and hybridized with a FITC-labeled PNA (CCCTAA)₃ probe, followed by quantifying TFUs in approximately 2,000 telomeres, with a telomere distribution curve being shown in C and F. (G and H) Telomere elongation in *PinX1*^{+/-} MEFs at late passage, as determined by telomere Southern blot. Multiple independent clones of *PinX1*^{+/+} and *PinX1*^{+/-} MEFs were cast into plug molds, lysed, and digested, followed by Southern blot analysis using a TTAGGG repeat as a probe. Prior to hybridization, the gels were stained with ethidium bromide to insure equal loading of total DNA, with a segment of the gels being shown in lower panels (G), with average TRF lengths from 3 independent MEF lines being quantified using ImageQuant (H). (I and J) Telomere elongation at old (10–13 months) (J), but not young age (6–10 weeks) (I) of *PinX1*^{+/-} mice, as determined by qFISH. (K and L) Telomere elongation at old, but not young age of *PinX1*^{+/-} mice, as determined by Southern blot analysis of splenocytes (K), with average TRF lengths from 5–6 littermates being quantified using ImageQuant (L). The lanes were run on the same gel, but were noncontiguous. ***P* < 0.01. Data are represented as mean ± SD.

not significantly different between *PinX1*^{+/+} and *PinX1*^{+/-} cells either at early or late passage, and very few p53BP1 foci were colocalized with telomeres (Supplemental Figure 4B). These results suggest that PinX1 heterozygous knockout may not significantly increase telomere-mediated DNA damage. These results might be expected because these cells contained elevated telomerase activity (Figure 2, G and H) and telomerase does not induce DNA damage, but rather improves DNA repair (35, 36).

Since elevated telomerase activity was also found in PinX1 heterozygous knockout mouse tissues (Figure 2, I and J), we determined whether the time-dependent effects of PinX1 on telomere lengths also occur in mice by comparing telomere lengths in spleen cells isolated from both young (6–10 weeks) and old (10–13 months) *PinX1*^{+/+} and *PinX1*^{+/-} littermates. As recently reported (58), both qFISH (Figure 3, I and J) and Southern blot (Figure 3, K and L) analyses consistently showed that older *PinX1*^{+/-} mice had shorter telomeres than younger mice and, more importantly, telomeres in *PinX1*^{+/-} mice did not show age-dependent shortening, but rather lengthening. Young *PinX1*^{+/+} and *PinX1*^{+/-} mice had similar TFUs (Figure 3I) and TRF lengths (Figure 3, K and L). However, older *PinX1*^{+/-} mice had increased TFUs and longer TRF lengths, with their average increases by 51% (Figure 3J) and 56% (Figure 3, K and L), respectively. In addition, PinX1 knockdown in SV40-immortalized MEFs (Figure 4D) also significantly increased telomerase activity (Figure 4E and Supplemental Figure 2C) and telomere length (Figure 4F), as described below. Of note, unlike *PinX1*^{+/-} or PinX1 shRNA MEFs at late passages (Figure 3F and Figure 4F), the entire telomere distribution curve in old *PinX1*^{+/-} splenocytes was not shifted to the right (Figure 3J), which might be expected given that total splenocytes contain many different cell populations and many of them are differentiated and do not have active telomerase. Thus, reducing PinX1 by either knockout or knockdown increases telomerase activity leading to telomere elongation in cells and mice, as shown in cancer cells or yeasts, respectively (45, 47).

PinX1 heterozygous knockout or knockdown leads to anaphase bridges and chromosome instability in MEFs. Given that PinX1 heterozygous knockout in MEFs activates telomerase activity, leading to telomere elongation, we wondered whether these phenotypes are

associated with any cell-cycle defects. To examine this possibility, we compared *PinX1*^{+/+} and *PinX1*^{+/-} primary MEFs at early and late passages and observed a strikingly notable phenotype in *PinX1*^{+/-} MEFs only at late passage; approximately 16% of these cells displayed prominent anaphase bridges and/or lagging chromosomes (Figure 4, A and B). In contrast, these phenotypes were very rarely found in *PinX1*^{+/+} MEFs at the same late passage or *PinX1*^{+/-} MEFs and *PinX1*^{+/+} MEFs at early passage (Figure 4, A and B). Consistent with such obvious abnormal chromosome separation, approximately 80% of *PinX1*^{+/-} MEFs at late passage also displayed prominent aneuploidy, having more or less than the normal 40 chromosomes (Figure 4C). The frequency of aneuploidy was approximately 10-fold higher than that in *PinX1*^{+/-} MEFs at early passage or in *PinX1*^{+/+} MEFs at early and late passages (Figure 4C). Thus PinX1 heterozygous knockout leads to abnormal chromosome separation at late passage.

To independently confirm that reducing PinX1 function affects chromosome separation during mitosis, we examined the effects of PinX1 knockdown in MEFs that have been immortalized by SV40. After being infected with lentiviruses expressing PinX1 shRNA or control viruses, stable cell pools were selected. PinX1 shRNA effectively knocked down *PinX1* mRNA in stable pools (Figure 4D). Significantly, PinX1 knockdown increased telomerase activity by approximately 3-fold at various concentrations examined (Figure 4E and Supplemental Figure 2C). Consistent with telomerase activation, telomeres were elongated after 20 passages, with the average TFUs being increased by approximately 98%, as compared with vector control (Figure 4F). The findings that PinX1 shRNA was more potent in activating telomerase and elongating telomeres (Figure 4, E and F) than PinX1 heterozygous knockout (Figure 2, G and H, and Figure 3F) are consistent with the fact that PinX1 shRNA was more effective in reducing PinX1 expression (Figure 4D and Figure 2D). More importantly, although these SV40 immortalized MEFs had a slightly higher rate of anaphase bridges than primary MEFs (Figure 4, B and G), as expected, PinX1 knockdown also significantly increased anaphase bridges at 20 passages, with about 33% of cells displaying anaphase bridges, 4- to 5-fold higher than vector controls (Figure 4G). These results together indicate that reducing PinX1 levels by heterozygous knockout or knockdown leads to abnormal chromosome separation.

To further confirm abnormal separation of mitotic chromosome in *PinX1*^{+/-} MEFs, we performed multicolor FISH (M-FISH) analysis because this procedure allows us to identify all individual chromosomes and their overall structures using a distinctly identifiable color spectrum. The number of a given chromosome varied from 0 to 4 depending on the individual cells and specific chromosomes (Figure 4H), further confirming aneuploidy (Figure 4C). Importantly, chromosome translocations were readily detected in *PinX1*^{+/-} MEFs at late passage (Figure 4, I and J). For example, chromosomes were translocated between the short arms of 2 different chromosomes, with each containing a centromere (Figure 4I), or between the long arms of 2 different chromosomes, with 1 containing a centromere (Figure 4J). Importantly, such chromosome abnormalities were rarely found in *PinX1*^{+/+} MEF at the same passage or *PinX1*^{+/-} MEFs at early passage (data not shown), as expected from a very low frequency of anaphase bridges and aneuploidy in these cells (Figure 4, B and C). Thus, PinX1 heterozygous knockout not only increases telomerase activation, but also leads to anaphase bridges and chromosome instability in MEFs.

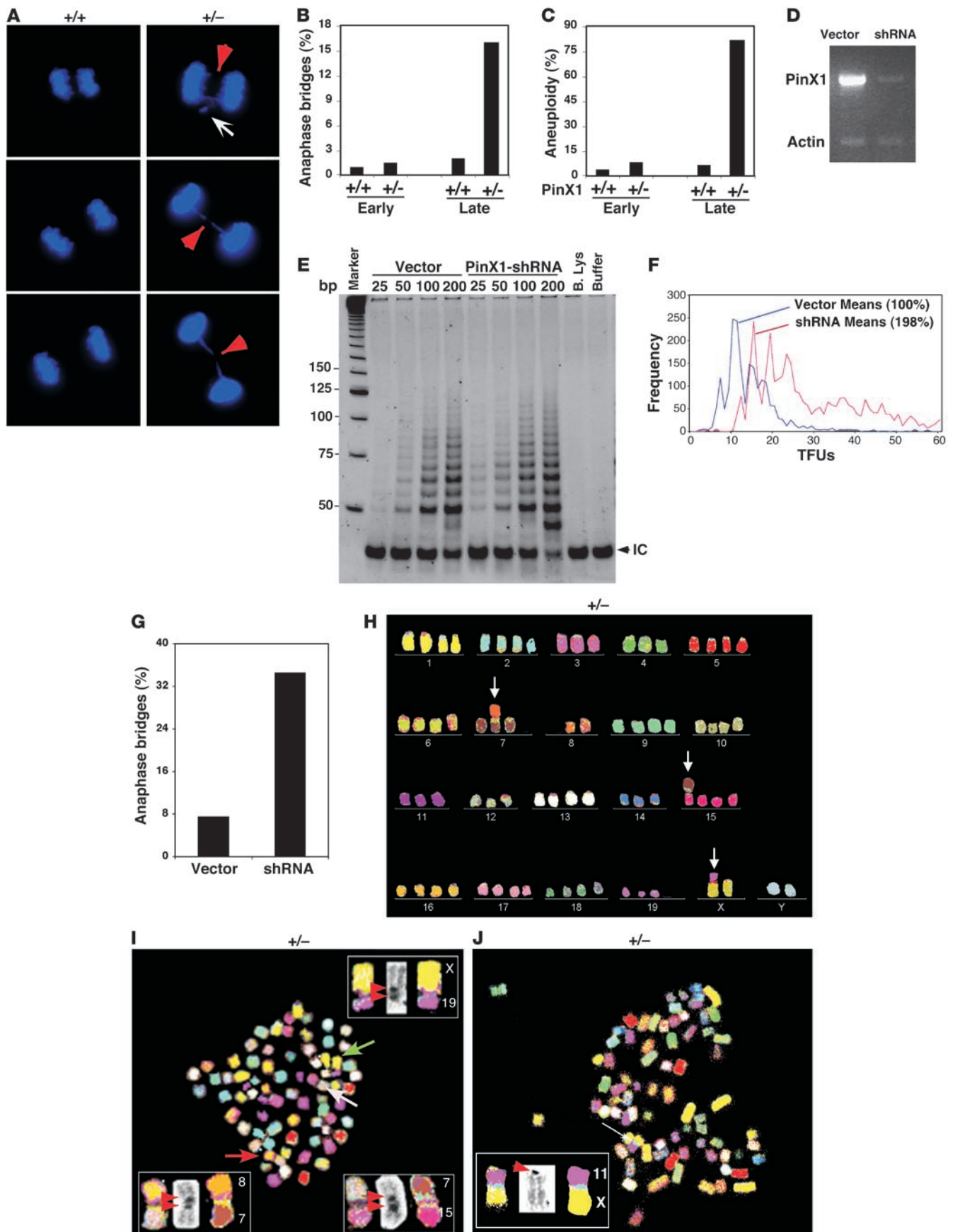


Figure 4

PinX1 heterozygous knockout or knockdown leads to anaphase bridges, lagging chromosomes, and chromosome instability in MEFs. (A–C) PinX1 knockout leads to anaphase bridges and chromosome instability at late passage. MEFs derived from *PinX1^{+/-}* and *PinX1^{+/-}* littermates were continuously cultured using the 3T3 protocol and fixed at early (from 3 to 5) or late (~30) passage, followed by staining with DAPI to score for the frequency of anaphase bridges and/or lagging chromosomes (A and B) and by counting the number of chromosomes at metaphase chromosome spreads to score for aneuploidy (C). (D–G) PinX1 knockdown leads to telomerase activation, telomere elongation, anaphase bridges, and chromosome instability at late passage. SV40 immortalized MEFs were stably infected with PinX1 shRNA or control viruses, followed by RT-PCR analysis (D) and TRAP assay using various amounts of telomerase-containing fractions (ng) (E) and semiquantified (Supplemental Figure 2C). Cells were continuously cultured, followed by analyzing telomere length using qFISH (F), anaphase bridges and/or lagging chromosomes at late (~20) passage (G). (H–J) Aneuploidy (H) and chromosome instability in *PinX1^{+/-}* MEFs (I and J) at late passages. Insets show examples of chromosome translocations (left to right), the display color, the inverted DAPI counterstain, and the classification pseudocolor. Arrows in I and J point to chromosome fusions, while red arrows in insets point to centrosomes. Numbers indicate the chromosomal origin of each fragment. Insets in I show 3 examples of translocations between short arms of 2 different chromosomes, with each containing a centromere, while inset in J shows an example of a translocation between long arms of 2 different chromosomes, with 1 containing a centromere.

TERT knockdown or knockout rescues telomerase activation and telomere elongation and also abrogates anaphase bridges and chromosome instability in PinX1^{+/-} MEFs. The above findings indicate that inhibiting endogenous PinX1 through gene knockout or knockdown in cells increases telomerase activity, leading to telomere elongation, anaphase bridges, and chromosome instability. Given that PinX1 is a telomerase inhibitor (45, 47–49), a key question is whether telomerase is essential for PinX1 ablation to affect telomere length and chromosome stability.

To address this question, we first knocked down TERT in *PinX1^{+/-}* MEFs to examine its effects on telomere length and chromosome instability. *PinX1^{+/-}* and *PinX1^{+/-}* MEFs were stably infected with lentiviruses expressing 2 different TERT-shRNA constructs at passage 3, before any chromosome instability phenotypes were observed. Both TERT-shRNA constructs effectively knocked down TERT mRNA (Figure 5A) and telomerase activity (Figure 5B and Supplemental Figure 2, D and E) in *PinX1^{+/-}* and *PinX1^{+/-}* MEFs. To examine the effects of telomerase knockdown on telomere length and chromosome instability, we continuously cultured stable cell pools in vitro for approximately 20 passages. Telomerase knockdown in *PinX1^{+/-}* MEFs did not have any detectable effects on telomere length, anaphase bridges, aneuploidy, or overall DNA content profile within the 20 passages examined (Figure 5C, Supplemental Figure 3, and data not shown). Importantly, although viral infection itself did not have any obvious effects on *PinX1^{+/-}* or *PinX1^{+/-}* MEFs (Figure 5, C and D, and Supplemental Figure 3), both TERT shRNAs almost fully suppressed telomere elongation (Figure 5, E and F), anaphase bridges (Figure 5G), and aneuploidy (Figure 5H) in *PinX1^{+/-}* cells. Moreover, TERT-silenced *PinX1^{+/-}* cells had DNA content similar to that of control diploid *PinX1^{+/-}* MEFs (Figure 5, K and L vs. I), whereas the DNA content in control *PinX1^{+/-}* cells lay between those of diploid and tetraploid cells

(Figure 5, J vs. I), which is consistent with M-FISH analysis (Figure 4, H–J). These results show that TERT knockdown almost completely abrogates the ability of PinX1 knockout to induce telomerase activation, telomere elongation, and chromosome instability in MEFs.

Since shRNA constructs could sometimes have off-target effects, we needed to use an independent method to examine the role of telomerase in mediating the PinX1 phenotypes. For this purpose, we crossed *PinX1^{+/-}* mice and *Tert^{-/-}* mice to isolate *Tert^{-/-}* MEFs in the presence or absence of PinX1 heterozygous knockout (Figure 5M), followed by measuring telomere length and anaphase bridges at early (from 3 to 5) and late (from 25 to 30) passages. PinX1 heterozygous knockout failed to induce any increase in telomere length (Figure 5, N and O) and anaphase bridges and/or lagging chromosomes (Figure 5P) in *Tert^{-/-}* MEFs even at late passage. Similarly, PinX1 knockdown failed to induce any obvious increase in anaphase bridges and/or lagging chromosomes in G1 *Tert^{-/-}* MEFs (Supplemental Figure 5). These results indicate that telomerase is essential for PinX1 to affect telomere length and chromosome instability and demonstrate that reducing PinX1 activates telomerase and leads to telomerase-dependent telomere elongation and chromosome instability.

Most PinX1 heterozygous knockout mice develop malignant tumors of varied histopathology, which are unusual in mice, but are known to have LOH at 8p23 in humans. The above results show that PinX1 is reduced in most human breast cancer tissues and cells and that reducing PinX1 increases telomerase activity, leading to telomere elongation and chromosome instability in cells. Although further experiments are needed to elucidate whether chromosome instability is related to telomere-dependent, and/or -independent functions of telomerase or PinX1, we have focused our effort on determining whether reducing PinX1 levels leads to cancer development. This question is important because PinX1 is located at 8p23 in humans, a frequent LOH region in many epithelial cancers, and depleting PinX1 increases tumorigenicity of cancer cells (8, 9, 45, 50). Moreover, it might offer new insights into the development and treatment of human cancers.

To address this question, we first monitored a group totaling 52 *PinX1^{+/-}* and 15 *PinX1^{+/-}* mice generated from intercrosses of young *PinX1^{+/-}* mice for tumor phenotypes (Supplemental Figure 6 and Supplemental Table 1). Whereas only 1 of 15 *PinX1^{+/-}* mice developed a liver tumor, strikingly, 49 out of 52 *PinX1^{+/-}* mice developed tumors at relatively young ages, mostly between 9 and 18 months (Table 2, Supplemental Figure 6, and Supplemental Table 1). Most tumors were epithelial carcinomas arising in organs that are known to develop common cancers in humans and also known to have frequent heterozygous loss at 8p23 in humans (Table 2). The most common tumors were lung cancer (37% of all tumors), followed by liver cancer (18%), mammary cancer (13%), and then tumors of the gastrointestinal tract (10%), including stomach, small intestine, colon, and rectum (Table 2 and Supplemental Table 1). Tumors were found in both sexes of *PinX1^{+/-}* mice that were generated from 2 independent clones of targeted ES cells (Supplemental Table 1). Most tumors showed features commonly seen in advanced human carcinomas such as nuclear atypia, desmoplasia, stromal invasion, and/or distant metastasis (Figure 6).

Notably, about one-fifth of *PinX1^{+/-}* mice developed more than 1 type of tumor, with 3 and 7 mice having 3 and 2 tumor types in the same animals, respectively (Supplemental Table 1 and Figure 6, A–J). Furthermore, there were diverse histopathologies observed

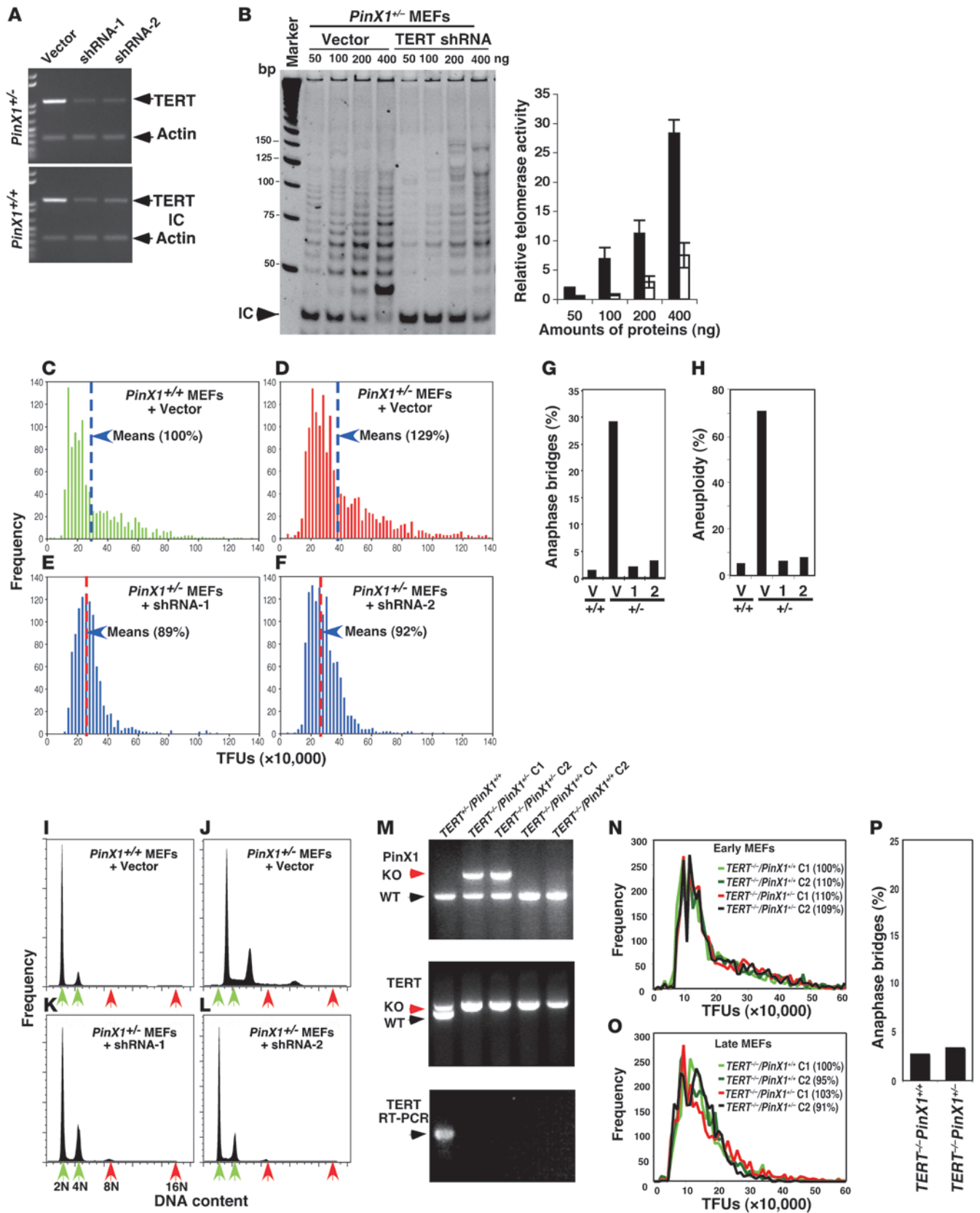


**Figure 5**

TERT knockdown or knockout rescues telomerase activation and telomere elongation and abrogates anaphase bridges and chromosome instability in *PinX1*^{+/-} MEFs. (A and B) TERT knockdown. *PinX1*^{+/+} and *PinX1*^{+/-} MEFs were stably infected with 2 different TERT shRNA or control lentiviruses, followed by quantitative TERT RT-PCR analysis with actin as a control (A) and TRAP assay (B, Supplemental Figure 2D, and E). Data are represented as mean ± SD. (C–F) TERT knockdown rescues telomere lengthening in *PinX1*^{+/-} MEFs at late passage. Stable cells were continuously cultured for 20 passages and then subjected to telomere qFISH. TERT knockdown had no effects on telomere length in *PinX1*^{+/+} MEFs under the same conditions (Supplemental Figure 3). (G and H) TERT knockdown rescues anaphase bridges, lagging chromosomes, and aneuploidy in *PinX1*^{+/-} MEFs. *PinX1*^{+/+} and *PinX1*^{+/-} MEFs expressing TERT shRNAs or control vector were fixed at 20 passages, followed by scoring for the frequency of anaphase bridges and/or lagging chromosomes (G) or aneuploidy (H). (I–L) TERT knockdown rescues abnormal DNA content in *PinX1*^{+/-} MEFs. *PinX1*^{+/+} and *PinX1*^{+/-} MEFs expressing TERT shRNAs or control were fixed at 20 passages, followed by flow cytometry to determine the DNA content. Green and red arrows point to the DNA contents expected for diploid and tetraploid cells, respectively. (M) Generation of TERT and PinX1 double-knockout MEFs. 2 MEF lines of each group derived from *Tert*^{-/-} and *PinX1*^{+/+} or *PinX1*^{+/-} embryos at E12.5 were subjected to PCR genotyping and confirmed by RT-PCR. (N and O) TERT knockout prevents telomere elongation in *PinX1*^{+/-} MEFs at late passage, as determined by qFISH. (P) TERT knockout prevents anaphase bridges and/or lagging chromosomes in *PinX1*^{+/-} MEFs at late passage.

in the same types of tumors among different mice or even in the same tumors (Figure 6). For example, in mammary adenocarcinomas, there were many different growth patterns (Figure 6, K–P). Furthermore, even in the same mice, mammary cancer cells displayed different differentiation states and tumor grades, including high (Figure 6N), intermediate (Figure 6O), and low (Figure 6P) grades of cancer cells. Similarly, even in the same lung cancer section, cancer cells with high (Figure 6R), intermediate (Figure 6S), and low (Figure 6T) tumor grades were located right next to each other. Finally, *PinX1*^{+/-} tumors developed lung metastasis from lung cancer (Figure 6I) or mammary cancer (Figure 6J). These results together indicate that almost all *PinX1*^{+/-} mice spontaneously develop aggressive epithelial tumors that are unusual in mice, but are common in humans, demonstrating strong tumor-suppressing function for PinX1.

Since telomerase knockout (33) or telomere deprotection (34) shifts the tumor spectrum of p53 mutant mice from mainly lymphoma to include epithelial carcinomas, similarly to TERT overexpression (31), we crossed *PinX1*^{+/-} mice with p53 knockout mice and examined the effects of PinX1 heterozygous knockout on the tumor spectrum of p53 knockout mice. As expected, p53 knockout mice mainly developed lymphoma (Table 3). However, in the presence of PinX1 heterozygous knockout, the frequency of epithelial carcinomas such as lung, liver, breast, and gastrointestinal cancers was dramatically increased both in p53 heterozygous and homozygous knockout mice, with most p53^{-/-} and *PinX1*^{+/-} mice dying of cancer between 6–9 months and most p53^{+/-} and *PinX1*^{+/-} mice between 9–12 months (Table 3), when the majority of *PinX1*^{+/-} mice just started to develop tumors (Supplemental Figure 6). These results indicate that PinX1 heterozygous knockout shifts the tumor spectrum of p53 mutant mice toward epithelial carcinomas.

PinX1 heterozygous knockout cancer cells express reduced PinX1 and display obvious telomere elongation, anaphase bridges, and chromosome instability. Given that PinX1 heterozygous knockout reduces PinX1 expression and activates telomerase, leading to aggressive epithelial malignancies in mice, we asked whether *PinX1*^{+/-} cancer cells have any PinX1 protein and any evidence of telomere elongation and chromosome instability.

To determine whether *PinX1*^{+/-} cancer cells express any PinX1 protein, we first analyzed PinX1 protein and mRNA levels in a large number of tumor samples and surrounding noncancerous samples of liver, lung, and mammary tissues in *PinX1*^{+/-} mice. Compared with levels in normal tissues of *PinX1*^{+/+} mice, levels of *PinX1* mRNA and protein were reduced to a similar extent (>50%) in cancer tissues and the surrounding noncancerous tissues in the *PinX1*^{+/-} mice (Figure 7, A–D, and data not shown), further supporting PinX1 haploinsufficiency.

To detect chromosome instability phenotypes in *PinX1*^{+/-} tumors, we first looked for anaphase bridges in lung and mammary tumors after staining their series sections with H&E. Anaphase bridges and/or lagging chromosomes were readily found in both tumors (Figure 7, E and F), with up to 10% of mitotic cells, depending on the angle of sectioning, suggesting that PinX1 mutant tumors might have chromosome instability. To further examine this possibility, we established primary cell cultures from *PinX1*^{+/-} lung and mammary tumors and their respective normal controls using the procedure we described earlier (59). Both types of cancer cells displayed telomere elongation, with the average TFU increased by approximately 2-fold (Figure 7, G and H), but also anaphase bridges and/or lagging chromosomes in approximately 30% of cells (data not shown). These results indicate that *PinX1*^{+/-} tumors displayed prominent anaphase bridges and/or lagging chromosomes, suggesting chromosome instability.

Table 2
PinX1 knockout mice develop a range of epithelial cancers

Genotype	Tumors
<i>PinX1</i>^{+/+} mice (n = 15)	
Tumor-negative mice	14 (93.2%)
Tumor-positive mice (liver cancer)	1 (6.8%)
<i>PinX1</i>^{+/-} mice (n = 52)	
Tumor-negative mice	3 (5.8%)
Tumor-positive mice	43 (94.2%)
Total primary tumors ^A	62 (100%)
Lung cancer ^B	23 (37.1%)
Liver cancer	11 (17.7%)
Mammary cancer ^B	8 (12.9%)
Gastrointestinal cancer	6 (9.7%)
Lymphoma	4 (6.5%)
Histiocytic sarcoma	2 (3.2%)
Eye Harderian gland adenoma	2 (3.2%)
Skin hyperplasia	2 (3.2%)
Hibernoma	1 (1.6%)
Undifferentiated sarcoma	1 (1.6%)
Angiosarcoma	1 (1.6%)
Leiomyocarcinoma	1 (1.6%)

^A7 mice had 2 tumor types and 3 mice had 3 tumor types. ^B2 mice with mammary cancer and 1 with lung cancer had lung metastasis.

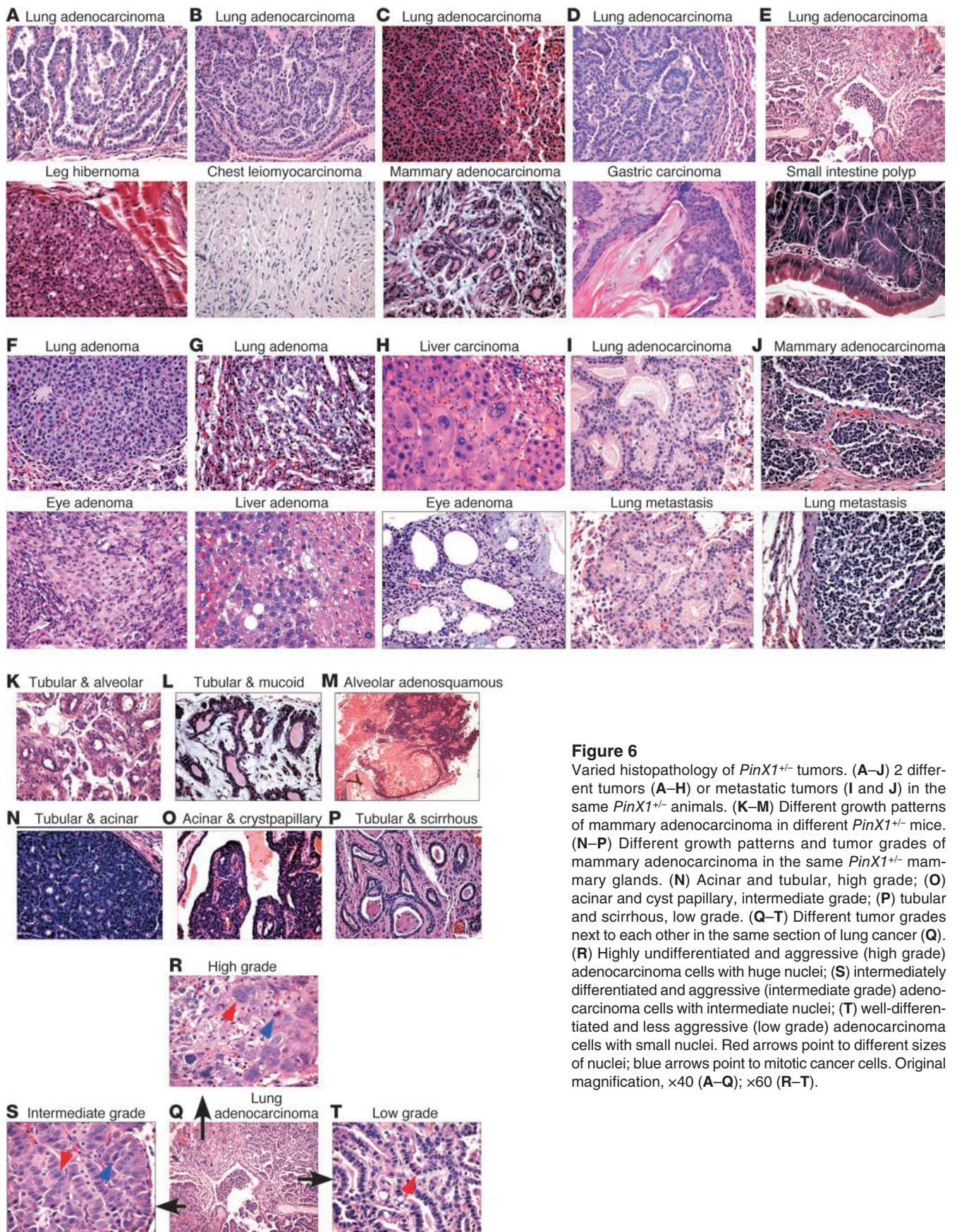


Figure 6

Varied histopathology of *PinX1*^{+/-} tumors. (A–J) 2 different tumors (A–H) or metastatic tumors (I and J) in the same *PinX1*^{+/-} animals. (K–M) Different growth patterns of mammary adenocarcinoma in different *PinX1*^{+/-} mice. (N–P) Different growth patterns and tumor grades of mammary adenocarcinoma in the same *PinX1*^{+/-} mammary glands. (N) Acinar and tubular, high grade; (O) acinar and cyst papillary, intermediate grade; (P) tubular and scirrhous, low grade. (Q–T) Different tumor grades next to each other in the same section of lung cancer (Q). (R) Highly undifferentiated and aggressive (high grade) adenocarcinoma cells with huge nuclei; (S) intermediately differentiated and aggressive (intermediate grade) adenocarcinoma cells with intermediate nuclei; (T) well-differentiated and less aggressive (low grade) adenocarcinoma cells with small nuclei. Red arrows point to different sizes of nuclei; blue arrows point to mitotic cancer cells. Original magnification, ×40 (A–Q); ×60 (R–T).



Table 3
PinX1 knockout shifts the tumor spectrum of p53 mutant mice toward epithelial carcinomas

Genotype	Tumors
<i>PinX1^{+/+}p53^{+/-}</i> mice (n = 14)	
Tumor-negative mice	3 (21.4%)
Tumor-positive mice	11 (78.6%)
Total primary tumors ^A	12 (100%)
Lymphoma	8 (66.6%)
Mammary cancer	2 (16.7%)
Skin cancer	2 (16.7%)
<i>PinX1^{+/-}p53^{+/-}</i> mice (n = 10)	
Tumor-negative mice	1 (10.0%)
Tumor-positive mice	9 (90.0%)
Total primary tumors ^B	11 (100%)
Liver cancer	3 (27.3%)
Lymphoma	3 (27.3%)
Lung cancer	2 (18.2%)
Mammary cancer	2 (18.2%)
Ovary cancer	1 (9.0%)
<i>PinX1^{+/+}p53^{-/-}</i> mice (n = 9)	
Tumor-negative mice	1 (11.1%)
Tumor-positive mice	8 (88.9%)
Total primary tumors	8 (100%)
Lymphoma	8 (100%)
<i>PinX1^{+/-}p53^{-/-}</i> mice (n = 6)	
Tumor-negative mice	0 (0%)
Tumor-positive mice	6 (100%)
Total primary tumors ^C	9 (100%)
Lymphoma	4 (44.4%)
Liver cancer	3 (33.4%)
Mammary cancer	1 (11.1%)
Gastrointestinal cancer	1 (11.1%)

^A1 mouse had 2 tumor types. ^B2 mice had 2 tumor types. ^C3 mice had 2 tumor types.

To obtain further evidence of chromosome instability in *PinX1^{+/-}* tumors, we performed genome-wide oligonucleotide-based array comparative genome hybridization (aCGH) analysis of 6 *PinX1^{+/-}* tumor samples and WT controls. Each sample was repeated twice by performing dye-swap experiments to ensure that red and blue signals showed reproducible mirror images, as expected for true chromosome imbalance, as shown previously (60). We observed widespread chromosomal imbalances with regions of gain or loss (Supplemental Figure 7), which were different among the samples analyzed. These results are consistent with the diverse chromosome instability in *PinX1^{+/-}* MEFs (Figure 4, H–J) and also with the diverse histopathologies of *PinX1^{+/-}* tumors (Figure 6). Importantly, mapping breakpoints with concomitant gain or loss among different chromosomes revealed many possible chromosome fusions. For example, the concomitant gains of 6qA1–A3.1 and 8qE2–8qD1 and remaining chromosome 8 (Figure 7I) or of 4qE1–18qA1 with breakpoints outside of these regions (Figure 7J) are consistent with chromosome fusions between 6q and 8q or between 4q and 18q, similar to chromosome fusions obtained from M-FISH analysis of *PinX1^{+/-}* MEFs (Figure 4, H–J). Thus, *PinX1^{+/-}* cancer cells

display prominent anaphase bridges and chromosome instability, as seen in *PinX1^{+/-}* MEFs, indicating that telomerase activity and chromosome instability likely contribute to tumorigenesis in *PinX1* mutant mice. These findings together indicate that *PinX1* heterozygous knockout increases telomerase activity and induces chromosome instability, eventually leading to the development of aggressive epithelial cancers in most mice.

Discussion

PinX1 is a conserved potent telomerase inhibitor, but its physiological or pathological function is largely unknown. We here show that *PinX1* expression is reduced in most human breast cancer tissues and cell lines examined. Importantly, reducing *PinX1* expression via heterozygous knockout or knockdown increases telomerase activity and leads to concomitant telomerase-dependent telomere elongation and chromosomal instability. Moreover, *PinX1* heterozygous knockout causes most mice to spontaneously develop a range of malignant tumors displaying evidence of telomere elongation and chromosomal instability. Notably, the majority of cancers in these mutant mice are carcinomas and share tissues of origin with human cancer types linked to 8p23 alterations. In addition, *PinX1* knockout also shifts the tumor spectrum of p53 mutant mice toward epithelial carcinomas. These results are, to our knowledge, the first demonstration that *PinX1* is a major haploinsufficient tumor suppressor and also provide what we believe is the first genetic evidence linking aberrant telomerase activation to chromosome instability, at least under the conditions where its endogenous inhibitor *PinX1* is reduced. These findings not only uncover what we believe is a novel role of *PinX1* and telomerase in chromosome instability and cancer initiation, but also suggest that telomerase inhibitors may be potentially effective in treating *PinX1*-related cancers.

PinX1 is a major haploinsufficient tumor suppressor at human chromosome 8p23. Human *PinX1* gene is located at 8p23 near the marker D8S277 (8, 45). This region has been widely investigated because it is a frequent LOH region in common human adult epithelial cancers (4–14), but major tumor suppressor or suppressors at this region remain to be identified. Our new results indicate that *PinX1* is a strong candidate for such a major tumor suppressor. We show that *PinX1* is reduced in most human breast cancer tissues and cell lines examined (Figure 1) and that *PinX1* expression is gene-dosage dependent; ablation of 1 allele reduces protein level by 60%–70% in vitro and in vivo (Figure 2). Furthermore, *PinX1* heterozygous knockout or knockdown not only increases telomerase activity (Figures 2 and 4E and Supplemental Figure 2, A–C) and telomere length (Figures 3 and 4F), but also leads to chromosome instability in cells (Figure 4). Furthermore, the resulting chromosome instability is dependent on aberrant telomerase activation (Figure 5). The significance of these findings is further substantiated by the demonstration that nearly all *PinX1* heterozygous knockout mice develop a range of epithelial malignancies (Figure 6 and Table 2) and that *PinX1* mutant cancer cells express reduced *PinX1* and display evidence of chromosome instability (Figure 7).

Although most human cancers are epithelial carcinomas, common tumor suppressor mutant mice mainly develop lymphomas and soft tissue sarcomas, with a few exceptions (61, 62). Notably, *PinX1^{+/-}* tumors are among the most common tumors and are also known to have frequent LOH at 8p23 in humans, including lung, breast, liver, and gastrointestinal cancers (Table 2). Moreover, many mutant mice developed 2 or even 3 different cancer types and

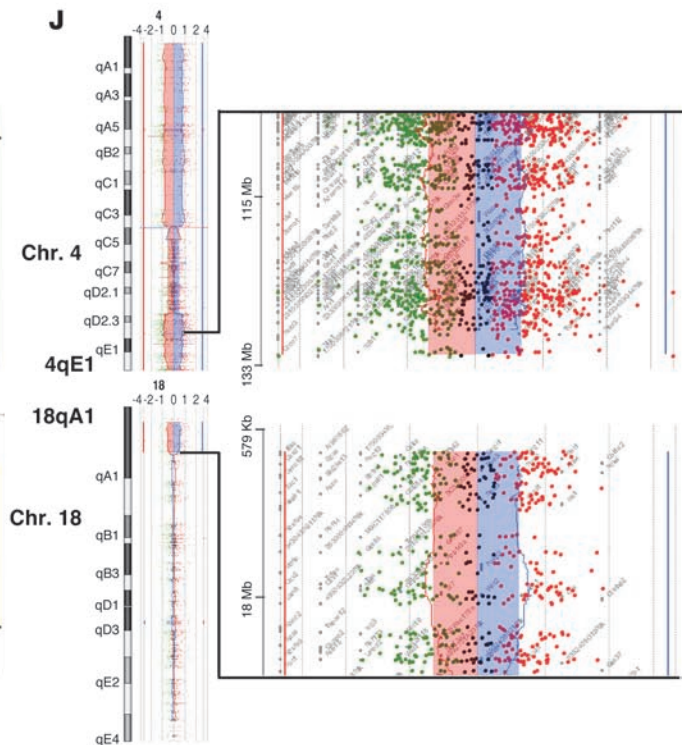
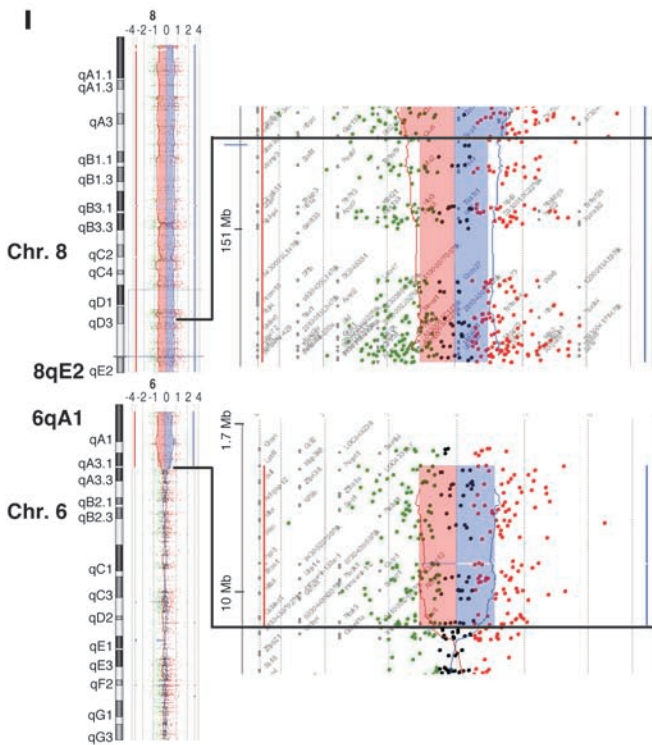
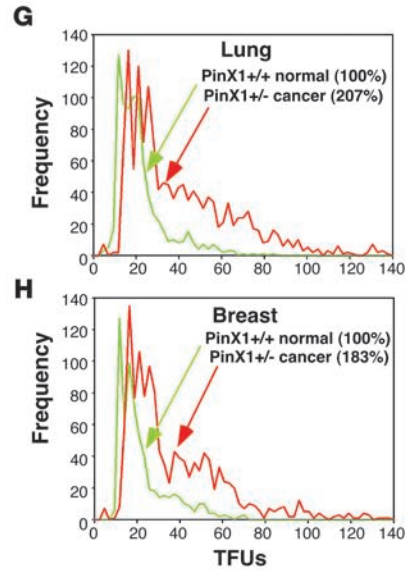
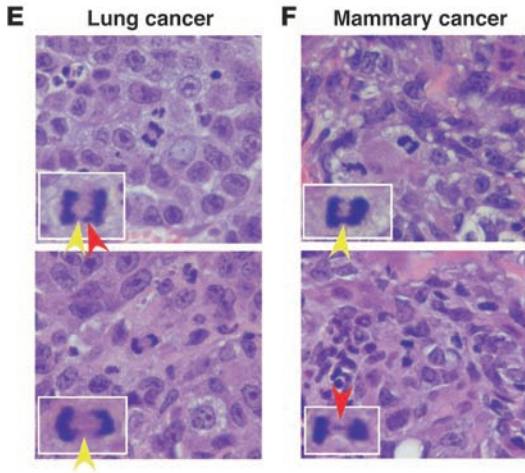
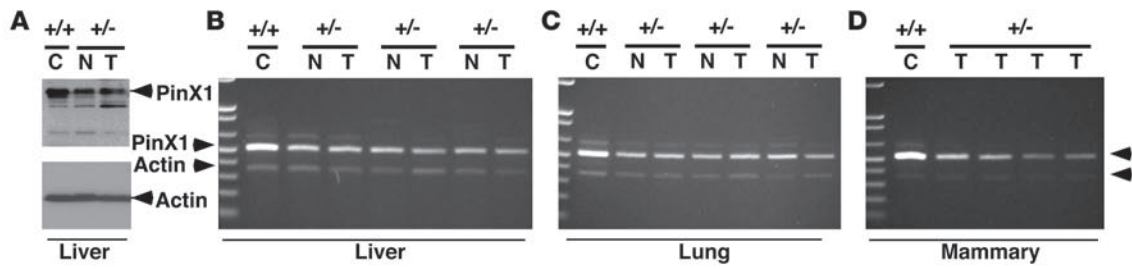


Figure 7

PinX1^{+/-} cancer cells express reduced PinX1 and display telomere elongation, anaphase bridges, lagging chromosomes, and chromosome instability. (A–D) Reduced PinX1 expression in *PinX1*^{+/-} tumors (T) at levels similar to those in the surrounding noncancerous tissues (N) of liver (A and B), lung (C), or mammary gland (D), or in *PinX1*^{+/+} normal control (C), as assayed by immunoblotting (A) or by qRT-PCR (B–D), with actin as a control. (E and F) Anaphase bridges and/or lagging chromosomes in *PinX1*^{+/-} lung and mammary tumors. H&E-stained serial sections of lung (E) or mammary tumors (F) were examined for anaphase bridges (yellow arrows) and/or lagging chromosomes (red arrows). Original magnification, ×100. (G and H) Telomere elongation in *PinX1*^{+/-} lung cancer cells and mammary cancer cells. *PinX1*^{+/-} primary lung (G) or mammary (H) cancer cells as well as their respective *PinX1*^{+/+} normal cells were subjected to qFISH. (I and J) Chromosome (Chr.) translocation in *PinX1*^{+/-} tumors. Genomic DNAs from *PinX1*^{+/-} tumors and *PinX1*^{+/+} normal tissues were subjected to aCGH analysis. Each sample was repeated twice by performing dye-swap experiments to make sure that red and blue signals showed reproducible mirror images. Aberration calls identified by the ADM-1 algorithm are shown. There were widespread chromosomal imbalances with regions of gain or loss, and altering gene copy number, with a 1 representative shown (Supplemental Figure 7). The concomitant gains of 6qA1-A3.1 and 8qE2-8qD1 and remaining chromosome 8 (I) or of 4qE1-18qA1 with breakpoints outside of these regions (J) are consistent with chromosome fusions between 6q and 8q or 4q and 18q.

metastases, and even within a given cancer type, histopathology varied among individuals and between and within tumors (Figure 6). This suggests that *PinX1*^{+/-} cancers likely originate from multiple cells and behave aggressively. These results are consistent with the findings that *PinX1* heterozygous knockout MEFs (Figure 4) and cancer cells (Figure 7) display widespread chromosome instability. Finally, *PinX1* heterozygous knockout also shifts the tumor spectrum of p53 mutant mice from lymphoma toward epithelial carcinomas (Table 3), similar to telomerase overexpression (31), telomerase knockout (33), or telomere deprotection (34). Notably, anaphase bridges, chromosome instability, and aneuploidy are very common in human cancers, especially epithelial tumors (63, 64). In addition, although telomere loss in cancers has been well studied, telomere elongation is quite common in human cancers, e.g., in more than 40% of liver cancer (65), esophageal cancer (66), and brain tumors (67), and also correlates with advanced stages and/or poor survival in some cancers (65, 66, 68, 69). Together with previous findings that reducing *PinX1* potently increases tumorigenicity of human cancer cells (45) and that *PinX1* is reduced in the majority of liver and gastric cancers (8, 9, 50), these results indicate that *PinX1* is a major haploinsufficient tumor suppressor whose reduction may contribute to tumorigenesis by activating telomerase and promoting chromosome instability. Given telomerase activation in most human cancers, loss of *PinX1* function likely contributes to the pathogenesis of many cancers and might have important therapeutic implications.

PinX1 is essential for inhibiting chromosome instability during tumorigenesis. The ability of *PinX1* to regulate telomerase is highly conserved from humans to yeasts (45–49). However, it is not known whether *PinX1* is a rate-limiting physiological regulator of telomerase and why such a negative regulatory mechanism is needed. We have now addressed these questions using *PinX1* knockout or knockdown in vitro and in vivo. Reduced *PinX1* expression by gene deletion or knockdown in MEFs increases telomerase activity, leading to telomere elongation, anaphase bridges, lagging chro-

mosomes, and chromosome instability (Figures 2–4). Moreover, TERT knockdown or knockout fully prevents *PinX1* deletion from not only activating telomerase activation and elongating telomeres, but also from inducing anaphase bridges and chromosome instability (Figure 5). Importantly, nearly all *PinX1*^{+/-} mice develop aggressive epithelial cancers that display elongated telomeres, anaphase bridges, lagging chromosomes, and chromosomal instability (Figures 6 and 7; Table 2). These results provide evidence for an essential role of *PinX1* in inhibiting telomerase activation and chromosome instability during tumorigenesis in vitro and in vivo. This is consistent with the critical role of *PinX1* in linking between TRF1 and telomerase inhibition to prevent telomere elongation and help maintain telomere homeostasis (46).

Telomerase is essential for PinX1 reduction to induce chromosome instability. At the present time, we do not yet know how reducing *PinX1* function leads to chromosome instability. Since *PinX1* localizes to nucleoli in addition to telomeres (45, 47) and affects some ribosomal RNA maturation in yeast (70), it could be possible, but less unlikely, that *PinX1* regulates chromosome stability via affecting some nucleolar function. Recently, Yuan et al. reported that exogenous *PinX1* binds to microtubules and localizes to kinetochores at mitosis and its almost complete knockdown in transient experiments causes chromosome mis-separation and micronuclei formation (71). At the first glance, these *PinX1* functions could explain chromosome instability in our *PinX1*-reduced cells. However, we observed abnormal cell division only when *PinX1* was almost completely knocked down or both *PinX1* alleles were deleted by infecting *PinX1*^{β/β} MEFs with CMV-Cre, and these cells died in a few days (data not shown). In contrast, *PinX1* heterozygous knockout or stable knockdown cells grew normally for an extended period before displaying anaphase bridges and chromosome instability. Therefore, *PinX1* action on the basic cellular structures might explain the essential function of *PinX1* for cell survival in MEFs and mice, and could contribute to chromosome instability, but cannot fully explain the phenotypes that we observed here due to partial *PinX1* reduction.

Notably, the *PinX1* knockout phenotypes including telomerase activation, telomere elongation, anaphase bridges, aneuploidy, and chromosome instability are fully suppressed by knockdown or knockout of TERT (Figure 5) or TERC (Supplemental Figure 5), indicating that telomerase is essential for *PinX1* reduction to induce chromosome instability. Moreover, it takes time for *PinX1*-induced telomerase activation to induce telomere elongation (Figure 3) and chromosome instability (Figure 4) when *PinX1* is knocked out or down. Notably, our *PinX1* and p53 double-mutant mice have a tumor spectrum similar to that found in TERC and p53 double-mutant mice due to telomere loss (33) or in TPP1/ACD and p53 double-mutant mice due to telomere deprotection (34). Furthermore, abnormal telomere elongation is common and also correlates with advanced stages and/or poor survival in some cancers (65, 66, 68, 69). Moreover, TERC is required for the tumor-promoting effects of TERT overexpression in transgenic mice (32). These results together suggest that abnormal telomerase activation and telomere elongation due to loss of *PinX1* might have effects on the development of epithelial cancers similar to those of telomere shortening or telomere deprotection. Given that *PinX1* directly binds to and inhibits TERT (45) and is targeted by TRF1 to telomeres to prevent abnormal telomere elongation by telomerase (46), it is conceivable that when *PinX1* is inhibited, telomerase is aberrantly activated without a proper brake and eventually leads to



chromosome instability, possibly via inducing aberrant telomere elongation to compromise telomere function. However, telomerase has other telomere-independent functions, such as is found in DNA damage response (35, 36) and activation of β -catenin (37). In addition, PinX1 might have nontelomeric functions such as in RNA maturation (70) and cell division (71). Therefore, further experiments are needed to define how PinX1 controls chromosome stability via telomere-dependent and/or -independent telomerase and/or other mechanisms unrelated to telomerase. Nevertheless, we have further demonstrated a major role of PinX1-induced chromosome instability in tumorigenesis.

We show that PinX1 is reduced in most human breast cancer tissues and cells (Figure 1) and that reducing PinX1 levels leads to telomerase activation, telomere elongation, and chromosome instability (Figures 2–4). Moreover, almost all PinX1 heterozygous knockout mice develop a range of epithelial malignancies, with multiple tumor types in the same mice, diverse cell morphologies/grades in 1 tumor type among mice, or even within individual tumors (Figures 6, and 7; Table 2). PinX1 heterozygous knockout also shifts the p53 mutant tumor spectrum to epithelial carcinomas (Table 3). Importantly, *PinX1*^{+/-} cancer cells also display chromosome instability (Figure 7) similar to that in PinX1-inhibited cells (Figure 4). Thus, PinX1 mutant tumors are likely derived from multiple epithelial cells, presumably due to chromosome instability. These results are consistent with previous findings that PinX1 potently controls tumorigenicity of cancer cells (45) and that telomerase overexpression is not as oncogenic as that in PinX1 knockout shown here. Analogous situations have been documented previously. For example, CDK subunit cyclin D1 overexpression in mice (72) is much less potent than CDK inhibitor p16 knockout in inducing tumorigenesis (73). Finally, our results also suggest that telomerase inhibition might be used to treat PinX1-related tumors.

In summary, we find that PinX1 is often reduced in human breast cancer, that reducing PinX1 leads to chromosome instability in a telomerase-dependent manner, and that PinX1 heterozygous knockout causes all mice to develop a range of malignancies with evidence of chromosome instability. Given that PinX1 is located at frequent LOH regions in many common human cancers and its expression is actually reduced in many breast, liver, and gastrointestinal tumors, these results indicate that low PinX1 can contribute to tumorigenesis by activating telomerase and inducing chromosome instability and suggest novel options for cancer treatments.

Methods

Analysis of *PinX1* expression. Levels of *PinX1* mRNA and protein were determined by qRT-PCR, immunoblotting, and immunocytochemistry (45), with the exception of using affinity-purified anti-PinX1 polyclonal antibodies that were raised against a GST-C-terminal 75-aa fragment of PinX1 in our laboratory, as described (45, 74). For detecting PinX1 expression in breast cancer tissues, serial sections of formalin-fixed and -embedded tissue microarrays (Imgenex) were immunostained, as described (74). PinX1 expression in each fixed breast cancer sample was semiquantified in a double-blind fashion as high, medium, or low according to the standards shown in Figure 1D.

Generation of *PinX1*^{+/-} mice and MEFs. The mouse *PinX1* gene was isolated from BAC clones and then subcloned into the pKOII vector provided by E. Li (Massachusetts General Hospital, Boston, Massachusetts, USA). Briefly, a 6-kb BamHI-NdeI fragment before the possible PinX1 promoter was

inserted into the XhoI site in front of the first loxP site as the 5' long arm, a 4-kb NdeI-BamHI fragment containing the possible PinX1 promoter and first exon between the first and second loxP sites, and a 2.3-kb BamHI-BamHI fragment containing a second exon behind the third loxP site as the 3' short arm. The vector was linearized with NotI and electroporated into AB2.1 ES cells, followed by selection with G418. Positive PinX1-targeted ES clones were screened by PCR genotyping using 4 different sets of primers and confirmed by genomic Southern blot analysis using DNA probes outside the 3' and 5' targeting sequences. Two clones, no. 201 and no. 345, had the correct rec of PinX1 targeting vector at the PinX1 locus. After injection into C57BL/6 blastocysts, ES clones 345 and 201 generated 9 and 2 chimeric mice, designated as A and B lines, respectively. Chimeric males were crossed with C57BL/6J females to generate *PinX1*^{rec/+} mice. *PinX1*^{rec/+} mice were intercrossed with CMV-Cre mice (53) (Jackson Laboratory) to generate *PinX1*^{-/-} mice. Primary MEFs were prepared from *PinX1*^{+/-} and *PinX1*^{-/-} embryos with or without TERT knockout at E12.5 produced from intercrosses of young *PinX1*^{+/-} mice and from crosses of *PinX1*^{+/-} mice and p53^{-/-} mice (Taconic) or *Tert*^{-/-} mice (75) (Mutant Mouse Regional Resource Centers, UCD) and maintained according to the 3T3 protocol, as described (56). All mice were in a C57BL/6/129Sv background, and the phenotypes were observed both in A and B lines of PinX1 mutant mice. All studies in animals were reviewed and approved by the institutional review board of Beth Israel Deaconess Medical Center.

Detection of telomerase activity. MEFs or mouse tissues were lysed, and telomerase-containing fraction was prepared, followed by measuring the telomerase activity using the standard TRAP assay, as described (45).

TRF length determination. TRF length analysis was performed as described (44). Briefly, splenocytes and MEFs were combined with an equal volume of 2% low melting point (LMP) agarose and cast into 100 μ l plug molds. Cells were lysed in a lithium dodecyl sulfate (LDS) solution, followed by digestion with HinfI and HaeIII restriction enzymes. Plugs were run on a 1% pulsed field-grade agarose gel and stained with EtBr, followed by drying down on filter paper and denaturing and neutralizing before being subjected to hybridization with a ³²P-(CCCTAA)₃ oligonucleotide probe. The average TRF length was calculated by quantifying the hybridization signals using ImageQuant.

qFISH. qFISH on cultured cells was performed as described (44), with the following modifications. Briefly, interphase cells grown on coverslips were fixed with 4% PFA. Cells were then hybridized with a FITC- or Cy3-(CCCTAA)₃ PNA probe (PerSeptive BioSystems) and stained with DAPI. After PNA hybridization, fluorescence signals were visualized under an epifluorescence microscope (Axiovert 200M; Zeiss) equipped with a computer piloted filter wheel. After localization of metaphases, blue (DAPI), red (Cy3), or green (FITC) fluorescence signals were captured. A flat-field template was used to correct for unevenness in field illumination. Original images were saved and used for quantitative analysis. TFUs were calculated with AxioVision 4.5 software (Zeiss). Approximately 2,000 telomere spots from each sample were used to collect telomere fluorescent-signal data.

Establishment of stable cells. To knock down PinX1 expression, SV40-immortalized MEFs or G1 *Tert*^{-/-} MEFs (provided by S. Chang at Yale University, New Haven, Connecticut, USA) were infected with lentiviruses encoding shRNA sequences against PinX1 (GTAGAAATAGACGC-CATACTA). To knock down TERT expression, *PinX1*^{+/-} and *PinX1*^{-/-} MEFs at passage 3 were infected with lentiviruses encoding shRNA sequences against 2 different mouse TERT sequences (shRNA-1, GCTCATTCTGT-CATCTACAAA; shRNA-2, GCTCAACTATGAGCGGACAAA) or control viruses provided by W. Hahn at Dana-Farber Cancer Institute (Boston, Massachusetts, USA). Stable cell pools were selected and analyzed for expression of the transgenes by immunoblotting analysis, qRT-PCR, and/or telomerase assay, as described (45).



Chromosome analysis in metaphase and anaphase cells. Metaphase cells were collected from a colcemid treatment and incubated in hypotonic buffer. After fixation in methanol/acidic acid, cells were dropped onto slides and stained with DAPI, followed by confocal microscopy. Anaphase cells were visualized by DAPI staining of cells grown on coverslips after fixation with 4% PFA.

Cytogenetics analysis. M-FISH analysis and genome-wide aCGH analysis were performed by Cytogenetics Core Facility at Dana-Farber/Harvard Cancer using the XCyte mFISH Kit (MetaSystems GmbH) and the Agilent Mouse Genome aCGH Microarray 44K Kit according to the manufacturers' protocol, respectively (60). Briefly, for M-FISH analysis, metaphase chromosome spreads were prepared and then hybridized with fluorescently labeled chromosome-specific DNA probes, followed by collecting chromosome images using a set of 5 fluorochrome-specific optic filters. For aCGH analysis, genomic DNA was isolated from *PinX1*^{+/+} tumors or age-matched *PinX1*^{+/+} normal controls, digested with restriction enzymes AluI and RsaI, and fluorescently labeled with Cy5 (test) and Cy3 (reference), followed by hybridization to 60-mer oligonucleotide microarrays. Dye-swap experiments (test in Cy3 and reference in Cy5) were performed for each sample. The arrays were scanned and analyzed using Agilent Software.

Histopathological analyses of tumors in *PinX1*^{+/+} mice. *PinX1*^{+/+} animals were intercrossed or crossed with *p53*^{+/+} mice (purchased from Taconic) to generate the experimental cohorts that were followed for the development of tumors. For histological sections, tissues were fixed and stained with H&E and then reviewed by the rodent histopathologist.

Statistics. Values are presented in percentages or as mean \pm SD, and differences between groups were analyzed by the Spearman's correlation test or 2-sided Student's *t* test, respectively. The Kaplan-Meier method was used

to estimate disease-free survival for *PinX1*^{+/+} and *PinX1*^{-/-} mice. The significance of the differences in disease-free survival among the cohorts was determined using the log-rank (Mantel-Cox) test. A *P* value of less than 0.05 was considered statistically significant.

Acknowledgments

We are grateful to L. Cantley, P.P. Pandolfi, B. Neel, and T. Hunter for constructive discussions; W. Hahn for many critical reagents and much advice; S. Chang for G1 *Terc*^{-/-} MEFs; E. Li and W. Yang for advice on generating *PinX1*-knockout mice; C. Lee's Cytogenetics Core for mFISH and CGH analyses; S. Hagen for Confocal Microscopy Core (NIH grant S10 RR017927); and the members of the Lu and Zhou laboratories for help or advice, especially J. Driver for editing the manuscript. The work was supported by NIH grant RO1CA122434 and Susan G. Komen for the Cure grant KG100958 to X.Z. Zhou.

Received for publication April 23, 2010, and accepted in revised form January 26, 2011.

Address correspondence to: Xiao Zhen Zhou or Kun Ping Lu, Department of Medicine, Beth Israel Deaconess Medical Center, Harvard Medical School, 330 Brookline Avenue, CLS 0408, Boston, Massachusetts 02215, USA. Phone: 617.735.2017 (X.Z. Zhou), 617.735.2016 (K.P. Lu); Fax: 617.735.2050; E-mail: xzhou@bidmc.harvard.edu (X.Z. Zhou), klu@bidmc.harvard.edu (K.P. Lu).

1. Foulkes WD. Inherited susceptibility to common cancers. *N Engl J Med.* 2008;359(20):2143–2153.
2. Nathanson KL, Wooster R, Weber BL. Breast cancer genetics: what we know and what we need. *Nat Med.* 2001;7(5):552–556.
3. Hartman AR, Ford JM. BRCA1 and p53: compensatory roles in DNA repair. *J Mol Med.* 2003;81(11):700–707.
4. Emi M, et al. Frequent loss of heterozygosity for loci on chromosome 8p in hepatocellular carcinoma, colorectal cancer, and lung cancer. *Cancer Res.* 1992;52(19):5368–5372.
5. Becker SA, Zhou YZ, Slagle BL. Frequent loss of chromosome 8p in hepatitis B virus-positive hepatocellular carcinomas from China. *Cancer Res.* 1996;56(21):5092–5097.
6. Nagai H, Pineau P, Tiollais P, Buendia MA, Dejean A. Comprehensive allelotyping of human hepatocellular carcinoma. *Oncogene.* 1997;14(24):2927–2933.
7. Pineau P, et al. Identification of three distinct regions of allelic deletions on the short arm of chromosome 8 in hepatocellular carcinoma. *Oncogene.* 1999;18(20):3127–3134.
8. Liao C, Zhao M, Song H, Uchida K, Yokoyama KK, Li T. Identification of the gene for a novel liver-related putative tumor suppressor at a high-frequency loss of heterozygosity region of chromosome 8p23 in human hepatocellular carcinoma. *Hepatology.* 2000;32(4 pt 1):721–727.
9. Kondo T, et al. Loss of heterozygosity and histone hypoacetylation of the PINX1 gene are associated with reduced expression in gastric carcinoma. *Oncogene.* 2005;24(1):157–164.
10. Kahng YS, Lee YS, Kim BK, Park WS, Lee JY, Kang CS. Loss of heterozygosity of chromosome 8p and 11p in the dysplastic nodule and hepatocellular carcinoma. *J Gastroenterol Hepatol.* 2003;18(4):430–436.
11. Yokota T, et al. Localization of a tumor suppressor gene associated with the progression of human breast carcinoma within a 1-cM interval of 8p22-p23.1. *Cancer.* 1999;85(2):447–452.
12. Loo LW, et al. Array comparative genomic hybridization analysis of genomic alterations in breast cancer subtypes. *Cancer Res.* 2004;64(23):8541–8549.
13. Bhattacharya N, et al. Three discrete areas within the chromosomal 8p21.3-23 region are associated with the development of breast carcinoma of Indian patients. *Exp Mol Pathol.* 2004;76(3):264–271.
14. Varma G, et al. Array comparative genomic hybridization (aCGH) analysis of premenopausal breast cancers from a nuclear fallout area and matched cases from Western New York. *Br J Cancer.* 2005;93(6):699–708.
15. Hamaguchi M, et al. DBC2, a candidate for a tumor suppressor gene involved in breast cancer. *Proc Natl Acad Sci U S A.* 2002;99(21):13647–13652.
16. Lai J, Flanagan J, Phillips WA, Chenevix-Trench G, Arnold J. Analysis of the candidate 8p21 tumour suppressor, BNIP3L, in breast and ovarian cancer. *Br J Cancer.* 2003;88(2):270–276.
17. Ishii H, et al. The FEZ1 gene at chromosome 8p22 encodes a leucine-zipper protein, and its expression is altered in multiple human tumors. *Proc Natl Acad Sci U S A.* 1999;96(7):3928–3933.
18. Kim NW, et al. Specific association of human telomerase activity with immortal cells and cancer. *Science.* 1994;266(5193):2011–2015.
19. Broccoli D, Young JW, de Lange T. Telomerase activity in normal and malignant hematopoietic cells. *Proc Natl Acad Sci U S A.* 1995;92(20):9082–9086.
20. Blackburn EH. Switching and signaling at the telomere. *Cell.* 2001;106(6):661–673.
21. Shay JW, Wright WE. Telomerase: a target for cancer therapeutics. *Cancer Cell.* 2002;2(4):257–265.
22. Maser RS, DePinho RA. Connecting chromosomes, crisis, and cancer. *Science.* 2002;297(5581):565–569.
23. Dong CK, Masutomi K, Hahn WC. Telomerase: regulation, function and transformation. *Crit Rev Oncol Hematol.* 2005;54(2):85–93.
24. Smogorzewska A, de Lange T. Regulation of telomerase by telomeric proteins. *Annu Rev Biochem.* 2004;73:177–208.
25. Blasco MA. Telomere length, stem cells and aging. *Nat Chem Biol.* 2007;3(10):640–649.
26. Hahn WC, Counter CM, Lundberg AS, Beijersbergen RL, Brooks M, Weinberg RA. Creation of human tumour cells with defined genetic elements. *Nature.* 1999;400(6743):464–468.
27. Bodnar AG, et al. Extension of life-span by introduction of telomerase into normal human cells. *Science.* 1998;279(5349):349–352.
28. Vaziri H, Benchimol S. Reconstitution of telomerase activity in normal human cells leads to elongation of telomeres and extended replicative life span. *Curr Biol.* 1998;8(5):279–282.
29. Gonzalez-Suarez E, et al. Increased epidermal tumors and increased skin wound healing in transgenic mice overexpressing the catalytic subunit of telomerase, mTERT, in basal keratinocytes. *EMBO J.* 2001;20(11):2619–2630.
30. Artandi SE, et al. Constitutive telomerase expression promotes mammary carcinomas in aging mice. *Proc Natl Acad Sci U S A.* 2002;99(12):8191–8196.
31. Gonzalez-Suarez E, Flores JM, Blasco MA. Cooperation between p53 mutation and high telomerase transgenic expression in spontaneous cancer development. *Mol Cell Biol.* 2002;22(20):7291–7301.
32. Cayuela ML, Flores JM, Blasco MA. The telomerase RNA component Terc is required for the tumour-promoting effects of Tert overexpression. *EMBO Rep.* 2005;6(3):268–274.
33. Artandi SE, et al. Telomere dysfunction promotes non-reciprocal translocations and epithelial cancers in mice. *Nature.* 2000;406(6796):641–645.
34. Else T, et al. Genetic p53 deficiency partially rescues the adrenocortical dysplasia phenotype at the expense of increased tumorigenesis. *Cancer Cell.* 2009;15(6):465–476.
35. Masutomi K, et al. The telomerase reverse transcriptase regulates chromatin state and DNA damage responses. *Proc Natl Acad Sci U S A.* 2005;102(23):8222–8227.
36. Sharma GG, et al. hTERT associates with human telomeres and enhances genomic stability and DNA repair. *Oncogene.* 2003;22(1):131–146.
37. Park JI, et al. Telomerase modulates Wnt signalling



- by association with target gene chromatin. *Nature*. 2009;460(7251):66–72.
38. Wang J, Xie LY, Allan S, Beach D, Hannon GJ. Myc activates telomerase. *Genes Dev*. 1998;12(12):1769–1774.
 39. Greenberg RA, et al. Telomerase reverse transcriptase gene is a direct target of c-Myc but is not functionally equivalent in cellular transformation. *Oncogene*. 1999;18(5):1219–1226.
 40. Wu KJ, et al. Direct activation of TERT transcription by c-MYC. *Nat Genet*. 1999;21(2):220–224.
 41. Lin SY, Elledge SJ. Multiple tumor suppressor pathways negatively regulate telomerase. *Cell*. 2003;113(7):881–889.
 42. van Steensel B, de Lange T. Control of telomere length by the human telomeric protein Trf1. *Nature*. 1997;385(6618):740–743.
 43. de Lange T. Shelterin: the protein complex that shapes and safeguards human telomeres. *Genes Dev*. 2005;19(18):2100–2110.
 44. Lee TH, et al. Essential role of Pin1 in the regulation of TRF1 stability and telomere maintenance. *Nat Cell Biol*. 2009;11(1):97–105.
 45. Zhou XZ, Lu KP. The Pin2/TRF1-interacting protein PinX1 is a potent telomerase inhibitor. *Cell*. 2001;107(3):347–359.
 46. Soohoo CY, Shi R, Lee TH, Huang P, Lu KP, Zhou XZ. Telomerase inhibitor PINX1 provides a link between TRF1 and telomerase to prevent telomere elongation. *J Biol Chem*. 2011;286(5):3894–3906.
 47. Lin J, Blackburn EH. Nucleolar protein PinX1p regulates telomerase by sequestering its protein catalytic subunit in an inactive complex lacking telomerase RNA. *Genes Dev*. 2004;18(4):387–396.
 48. Oh BK, Yoon SM, Lee CH, Park YN. Rat homolog of PinX1 is a nucleolar protein involved in the regulation of telomere length. *Gene*. 2007;400(1–2):35–43.
 49. Sun C, Wu Z, Jia F, Wang Y, Li T, Zhao M. Identification of zebrafish LPTS: a gene with similarities to human LPTS/PinX1 that inhibits telomerase activity. *Gene*. 2008;420(1):90–98.
 50. Park WS, et al. Genetic analysis of the liver putative tumor suppressor (LPTS) gene in hepatocellular carcinomas. *Cancer Lett*. 2002;178(2):199–207.
 51. Oh BK, Chae KJ, Park C, Park YN. Molecular analysis of PinX1 in human hepatocellular carcinoma. *Oncol Rep*. 2004;12(4):861–866.
 52. Hawkins GA, et al. Mutational analysis of PINX1 in hereditary prostate cancer. *Prostate*. 2004;60(4):298–302.
 53. Lewandoski M, Martin GR. Cre-mediated chromosome loss in mice. *Nat Genet*. 1997;17(2):223–225.
 54. Karlseder J, et al. Targeted deletion reveals an essential function for the telomere length regulator Trf1. *Mol Cell Biol*. 2003;23(18):6533–6541.
 55. Chiang YJ, Kim SH, Tessarollo L, Campisi J, Hodes RJ. Telomere-associated protein TIN2 is essential for early embryonic development through a telomerase-independent pathway. *Mol Cell Biol*. 2004;24(15):6631–6634.
 56. Liou YC, et al. Loss of Pin1 function in the mouse causes phenotypes resembling cyclin D1-null phenotypes. *Proc Natl Acad Sci U S A*. 2002;99(3):1335–1340.
 57. Takai H, Smogorzewska A, de Lange T. DNA damage foci at dysfunctional telomeres. *Curr Biol*. 2003;13(17):1549–1556.
 58. Flores I, Canela A, Vera E, Tejera A, Cotsarelis G, Blasco MA. The longest telomeres: a general signature of adult stem cell compartments. *Genes Dev*. 2008;22(5):654–667.
 59. Wulf G, Garg P, Liou YC, Iglehart D, Lu KP. Modeling breast cancer in vivo and ex vivo reveals an essential role of Pin1 in tumorigenesis. *EMBO J*. 2004;23(16):3397–3407.
 60. Perry GH, et al. The fine-scale and complex architecture of human copy-number variation. *Am J Hum Genet*. 2008;82(3):685–695.
 61. Wu X, Pandolfi PP. Mouse models for multistep tumorigenesis. *Trends Cell Biol*. 2001;11(11):S2–S9.
 62. Hakem R, Mak TW. Animal models of tumor-suppressor genes. *Annu Rev Genet*. 2001;35:209–241.
 63. Rudolph KL, Millard M, Bosenberg MW, DePinho RA. Telomere dysfunction and evolution of intestinal carcinoma in mice and humans. *Nat Genet*. 2001;28(2):155–159.
 64. Stewenius Y, et al. Defective chromosome segregation and telomere dysfunction in aggressive Wilms' tumors. *Clin Cancer Res*. 2007;13(22 pt 1):6593–6602.
 65. Oh BK, et al. High telomerase activity and long telomeres in advanced hepatocellular carcinomas with poor prognosis. *Lab Invest*. 2008;88(2):144–152.
 66. Gertler R, Doll D, Maak M, Feith M, Rosenberg R. Telomere length and telomerase subunits as diagnostic and prognostic biomarkers in Barrett carcinoma. *Cancer*. 2008;112(10):2173–2180.
 67. Nurnberg P, Thiel G, Weber F, Epplen JT. Changes of telomere lengths in human intracranial tumours. *Hum Genet*. 1993;91(2):190–192.
 68. Bisoffi M, Heaphy CM, Griffith JK. Telomeres: prognostic markers for solid tumors. *Int J Cancer*. 2006;119(10):2255–2260.
 69. Gertler R, et al. Telomere length and human telomerase reverse transcriptase expression as markers for progression and prognosis of colorectal carcinoma. *J Clin Oncol*. 2004;22(10):1807–1814.
 70. Guglielmi B, Werner M. The yeast homolog of human PinX1 is involved in rRNA and small nucleolar RNA maturation, not in telomere elongation inhibition. *J Biol Chem*. 2002;277(38):35712–35719.
 71. Yuan K, et al. PinX1 is a novel microtubule-binding protein essential for accurate chromosome segregation. *J Biol Chem*. 2009;284(34):23072–23082.
 72. Wang TC, Cardiff RD, Zukerberg L, Lees E, Arnold A, Schmidt EV. Mammary hyperplasia and carcinoma in MMTV-cyclin D1 transgenic mice. *Nature*. 1994;369(6482):669–671.
 73. Sharpless NE, et al. Loss of p16Ink4a with retention of p19Arf predisposes mice to tumorigenesis. *Nature*. 2001;413(6851):86–91.
 74. Wulf GM, Ryo A, Wulf GG, Lee SW, Niu T, Lu KP. Pin1 is overexpressed in breast cancer and potentiates the transcriptional activity of phosphorylated c-Jun towards the cyclin D1 gene. *EMBO J*. 2001;20(13):3459–3472.
 75. Liu Y, et al. The telomerase reverse transcriptase is limiting and necessary for telomerase function in vivo. *Curr Biol*. 2000;10(22):1459–1462.